Scaling Properties of Azimuthal Anisotropy in Au + Au and Cu + Cu Collisions at $\sqrt{s_{NN}} = 200$ GeV

A. Adare,[8] S. Afanasiev,[22] C. Aidala,[9] N. N. Ajitanand,[49] Y. Akiba,[43,44] H. Al-Bataineh,[38] J. Alexander,[49] A. Al-Jamel,[38] K. Aoki,[28,43] L. Aphecetche,[51] R. Armendariz,[38] S. H. Aronson,[3] J. Asai,[44] E. T. Atomssa,[29] R. Averbeck,[50] T. C. Awes,[39] B. Azmoun,[3] V. Babintsev,[18] G. Baksay,[14] L. Baksay,[14] A. Baldisseri,[11] K. N. Barish,[4] P. D. Barnes,[31] B. Bassalleck,[37] S. Bathe,[4] S. Batsouli,[9,39] V. Baublis,[42] F. Bauer,[4] A. Bazilevsky,[3] S. Belikov,[3,21] R. Bennett,[50] Y. Berdnikov,[46] A. A. Bickley,[8] M. T. Bjorndal,[9] J. G. Boissevain,[31] H. Borel,[11] K. Boyle,[50] M. L. Brooks,[31] D. S. Brown,[38] D. Bucher,[34] H. Buesching,[3] V. Bumazhnov,[18] G. Bunce,[3,44] J. M. Burward-Hoy,[31] S. Butsyk,[31,50] S. Campbell,[50] J.-S. Chai,[23] B. S. Chang,[58] J.-L. Charvet,[11] S. Chernichenko,[18] J. Chiba,[24] C. Y. Chi,[9] M. Chiu,[9,19] I. J. Choi,[58] T. Chujo,[55] P. Chung,[49] A. Churyn,[18] V. Cianciolo,[39] C. R. Cleven,[16] Y. Cobigo,[11] B. A. Cole,[9] M. P. Comets,[40] P. Constantin,[21,31] M. Csanád,[13] T. Csörgő,[25] T. Dahms,[50] K. Das,[15] G. David,[3] M. B. Deaton,[1] K. Dehmelt,[14] H. Delagrange,[51] A. Denisov,[18] D. d'Enterria,[9] A. Deshpande,[44,50] E. J. Desmond,[3] O. Dietzsch,[47] A. Dion,[50] M. Donadelli,[47] J. L. Drachenberg,[1] O. Drapier,[29] A. Drees,[50] A. K. Dubey,[57] A. Durum,[18] V. Dzhordzhadze,[4,52] Y. V. Efremenko,[39] J. Egdemir,[50] F. Ellinghaus,[8] W. S. Emam,[4] A. Enokizono,[17,30] H. En'yo,[43,44] B. Espagnon,[40] S. Esumi,[54] K. O. Eyser,[4] D. E. Fields,[37,44] M. Finger,[5,22] M. Finger, Jr.,[5,22] F. Fleuret,[29] S. L. Fokin,[27] B. Forestier,[32] Z. Fraenkel,[57] J. E. Frantz,[9,50] A. Franz,[3] A. D. Frawley,[15] K. Fujiwara,[43] Y. Fukao,[28,43] S.-Y. Fung,[4] T. Fusayasu,[36] S. Gadrat,[32] I. Garishvili,[52] F. Gastineau,[51] M. Germain,[51] A. Glenn,[8,52] H. Gong,[50] M. Gonin,[29] J. Gosset,[11] Y. Goto,[43,44] R. Granier de Cassagnac,[29] N. Grau,[21] S. V. Greene,[55] M. Grosse Perdekamp,[19,44] T. Gunji,[7] H.-Å. Gustafsson,[33] T. Hachiya,[17,43] A. Hadj Henni,[51] C. Haegemann,[37] J. S. Haggerty,[3] M. N. Hagiwara,[1] H. Hamagaki,[7] R. Han,[41] H. Harada,[17] E. P. Hartouni,[30] K. Haruna,[17] M. Harvey,[3] E. Haslum,[33] K. Hasuko,[43] R. Hayano,[7] M. Heffner,[30] T. K. Hemmick,[50] T. Hester,[4] J. M. Heuser,[43] X. He,[16] H. Hiejima,[19] J. C. Hill,[21] R. Hobbs,[37] M. Hohlmann,[14] M. Holmes,[55] W. Holzmann,[49] K. Homma,[17] B. Hong,[26] T. Horaguchi,[43,53] D. Hornback,[52] M. G. Hur,[23] T. Ichihara,[43,44] K. Imai,[28,43] M. Inaba,[54] Y. Inoue,[45,43] D. Isenhower,[1] L. Isenhower,[1] M. Ishihara,[43] T. Isobe,[7] M. Issah,[49] A. Isupov,[22] B. V. Jacak,[50] J. Jia,[9] J. Jin,[9] O. Jinnouchi,[44] B. M. Johnson,[3] K. S. Joo,[35] D. Jouan,[40] F. Kajihara,[7,43] S. Kametani,[7,56] N. Kamihara,[43,53] J. Kamin,[50] M. Kaneta,[44] J. H. Kang,[58] H. Kano,[43] H. Kanou,[43,53] T. Kawagishi,[54] D. Kawall,[44] A. V. Kazantsev,[27] S. Kelly,[8] A. Khanzadeev,[42] J. Kikuchi,[56] D. H. Kim,[35] D. J. Kim,[58] E. Kim,[48] Y.-S. Kim,[23] E. Kinney,[8] A. Kiss,[13] E. Kistenev,[3] A. Kiyomichi,[43] J. Klay,[30] C. Klein-Boesing,[34] L. Kochenda,[42] V. Kochetkov,[18] B. Komkov,[42] M. Konno,[54] D. Kotchetkov,[4] A. Kozlov,[57] A. Král,[10] A. Kravitz,[9] P. J. Kroon,[3] J. Kubart,[5,20] G. J. Kunde,[31] N. Kurihara,[7] K. Kurita,[45,43] M. J. Kweon,[26] Y. Kwon,[52,58] G. S. Kyle,[38] R. Lacey,[49] Y.-S. Lai,[9] J. G. Lajoie,[21] A. Lebedev,[21] Y. Le Bornec,[40] S. Leckey,[50] D. M. Lee,[31] M. K. Lee,[58] T. Lee,[48] M. J. Leitch,[31] M. A. L. Leite,[47] B. Lenzi,[47] H. Lim,[48] T. Liška,[10] A. Litvinenko,[22] M. X. Liu,[31] X. Li,[6] X. H. Li,[4] B. Love,[55] D. Lynch,[3] C. F. Maguire,[55] Y. I. Makdisi,[3] A. Malakhov,[22] M. D. Malik,[37] V. I. Manko,[27] Y. Mao,[41,43] L. Mašek,[5,20] H. Masui,[54] F. Matathias,[9,50] M. C. McCain,[19] M. McCumber,[50] P. L. McGaughey,[31] Y. Miake,[54] P. Mikeš,[5,20] K. Miki,[54] T. E. Miller,[55] A. Milov,[50] S. Mioduszewski,[3] G. C. Mishra,[16] M. Mishra,[2] J. T. Mitchell,[3] M. Mitrovski,[49] A. Morreale,[4] D. P. Morrison,[3] J. M. Moss,[31] T. V. Moukhanova,[27] D. Mukhopadhyay,[55] J. Murata,[45,43] S. Nagamiya,[24] Y. Nagata,[54] J. L. Nagle,[8] M. Naglis,[57] I. Nakagawa,[43,44] Y. Nakamiya,[17] T. Nakamura,[17] K. Nakano,[43,53] J. Newby,[30] M. Nguyen,[50] B. E. Norman,[31] A. S. Nyanin,[27] J. Nystrand,[33] E. O'Brien,[3] S. X. Oda,[7] C. A. Ogilvie,[21] H. Ohnishi,[43] I. D. Ojha,[55] H. Okada,[28,43] K. Okada,[44] M. Oka,[54] O. O. Omiwade,[1] A. Oskarsson,[33] I. Otterlund,[33] M. Ouchida,[17] K. Ozawa,[7] R. Pak,[3] D. Pal,[55] A. P. T. Palounek,[31] V. Pantuev,[50] V. Papavassiliou,[38] J. Park,[48] W. J. Park,[26] S. F. Pate,[38] H. Pei,[21] J.-C. Peng,[19] H. Pereira,[11] V. Peresedov,[22] D. Yu. Peressounko,[27] C. Pinkenburg,[3] R. P. Pisani,[3] M. L. Purschke,[3] A. K. Purwar,[31,50] H. Qu,[16] J. Rak,[21,37] A. Rakotozafindrabe,[29] I. Ravinovich,[57] K. F. Read,[39,52] S. Rembeczki,[14] M. Reuter,[50] K. Reygers,[34] V. Riabov,[42] Y. Riabov,[42] G. Roche,[32] A. Romana,[29,*] M. Rosati,[21] S. S. E. Rosendahl,[33] P. Rosnet,[32] P. Rukoyatkin,[22] V. L. Rykov,[43] S. S. Ryu,[58] B. Sahlmueller,[34] N. Saito,[28,43,44] T. Sakaguchi,[3,7,56] S. Sakai,[54] H. Sakata,[17] V. Samsonov,[42] H. D. Sato,[28,43] S. Sato,[3,24,54] S. Sawada,[24] J. Seele,[8] R. Seidl,[19] V. Semenov,[18] R. Seto,[4] D. Sharma,[57] T. K. Shea,[3] I. Shein,[18] A. Shevel,[42,49] T.-A. Shibata,[43,53] K. Shigaki,[17] M. Shimomura,[54] T. Shohjoh,[54] K. Shoji,[28,43] A. Sickles,[50] C. L. Silva,[47] D. Silvermyr,[39] C. Silvestre,[11] K. S. Sim,[26] C. P. Singh,[2] V. Singh,[2] S. Skutnik,[21] M. Slunečka,[5,22] W. C. Smith,[1] A. Soldatov,[18] R. A. Soltz,[30] W. E. Sondheim,[31] S. P. Sorensen,[52] I. V. Sourikova,[3] F. Staley,[11] P. W. Stankus,[39] E. Stenlund,[33] M. Stepanov,[38] A. Ster,[25] S. P. Stoll,[3] T. Sugitate,[17] C. Suire,[40] J. P. Sullivan,[31] J. Sziklai,[25] T. Tabaru,[44] S. Takagi,[54] E. M. Takagui,[47] A. Taketani,[43,44] K. H. Tanaka,[24] Y. Tanaka,[36] K. Tanida,[43,44] M. J. Tannenbaum,[3] A. Taranenko,[49] P. Tarján,[12] T. L. Thomas,[37]

M. Togawa,[28,43] A. Toia,[50] J. Tojo,[43] L. Tomášek,[20] H. Torii,[43] R. S. Towell,[1] V-N. Tram,[29] I. Tserruya,[57] Y. Tsuchimoto,[17,43] S. K. Tuli,[2] H. Tydesjö,[33] N. Tyurin,[18] C. Vale,[21] H. Valle,[55] H. W. van Hecke,[31] J. Velkovska,[55] R. Vertesi,[12] A. A. Vinogradov,[27] M. Virius,[10] V. Vrba,[20] E. Vznuzdaev,[42] M. Wagner,[28,43] D. Walker,[50] X. R. Wang,[38] Y. Watanabe,[43,44] J. Wessels,[34] S. N. White,[3] N. Willis,[40] D. Winter,[9] C. L. Woody,[3] M. Wysocki,[8] W. Xie,[4,44] Y. L. Yamaguchi,[56] A. Yanovich,[18] Z. Yasin,[4] J. Ying,[16] S. Yokkaichi,[43,44] G. R. Young,[39] I. Younus,[37] I. E. Yushmanov,[27] W. A. Zajc,[9,†] O. Zaudtke,[34] C. Zhang,[9,39] S. Zhou,[6] J. Zimányi,[25,*] and L. Zolin[22]

(PHENIX Collaboration)

[1]*Abilene Christian University, Abilene, Texas 79699, USA*
[2]*Department of Physics, Banaras Hindu University, Varanasi 221005, India*
[3]*Brookhaven National Laboratory, Upton, New York 11973-5000, USA*
[4]*University of California–Riverside, Riverside, California 92521, USA*
[5]*Charles University, Ovocný trh 5, Praha 1, 116 36, Prague, Czech Republic*
[6]*China Institute of Atomic Energy (CIAE), Beijing, People's Republic of China*
[7]*Center for Nuclear Study, Graduate School of Science, University of Tokyo, 7-3-1 Hongo, Bunkyo, Tokyo 113-0033, Japan*
[8]*University of Colorado, Boulder, Colorado 80309, USA*
[9]*Columbia University, New York, New York 10027, USA, and Nevis Laboratories, Irvington, New York 10533, USA*
[10]*Czech Technical University, Zikova 4, 166 36 Prague 6, Czech Republic*
[11]*Dapnia, CEA Saclay, F-91191, Gif-sur-Yvette, France*
[12]*Debrecen University, H-4010 Debrecen, Egyetem tér 1, Hungary*
[13]*ELTE, Eötvös Loránd University, H - 1117 Budapest, Pázmány P. s. 1/A, Hungary*
[14]*Florida Institute of Technology, Melbourne, Florida 32901, USA*
[15]*Florida State University, Tallahassee, Florida 32306, USA*
[16]*Georgia State University, Atlanta, Georgia 30303, USA*
[17]*Hiroshima University, Kagamiyama, Higashi-Hiroshima 739-8526, Japan*
[18]*IHEP Protvino, State Research Center of Russian Federation, Institute for High Energy Physics, Protvino, 142281, Russia*
[19]*University of Illinois at Urbana-Champaign, Urbana, Illinois 61801, USA*
[20]*Institute of Physics, Academy of Sciences of the Czech Republic, Na Slovance 2, 182 21 Prague 8, Czech Republic*
[21]*Iowa State University, Ames, Iowa 50011, USA*
[22]*Joint Institute for Nuclear Research, 141980 Dubna, Moscow Region, Russia*
[23]*KAERI, Cyclotron Application Laboratory, Seoul, South Korea*
[24]*KEK, High Energy Accelerator Research Organization, Tsukuba, Ibaraki 305-0801, Japan*
[25]*KFKI Research Institute for Particle and Nuclear Physics of the Hungarian Academy of Sciences (MTA KFKI RMKI), H-1525 Budapest 114, P.O. Box 49, Budapest, Hungary*
[26]*Korea University, Seoul, 136-701, Korea*
[27]*Russian Research Center "Kurchatov Institute," Moscow, Russia*
[28]*Kyoto University, Kyoto 606-8502, Japan*
[29]*Laboratoire Leprince-Ringuet, Ecole Polytechnique, CNRS-IN2P3, Route de Saclay, F-91128, Palaiseau, France*
[30]*Lawrence Livermore National Laboratory, Livermore, California 94550, USA*
[31]*Los Alamos National Laboratory, Los Alamos, New Mexico 87545, USA*
[32]*LPC, Université Blaise Pascal, CNRS-IN2P3, Clermont-Fd, 63177 Aubiere Cedex, France*
[33]*Department of Physics, Lund University, Box 118, SE-221 00 Lund, Sweden*
[34]*Institut für Kernphysik, University of Muenster, D-48149 Muenster, Germany*
[35]*Myongji University, Yongin, Kyonggido 449-728, Korea*
[36]*Nagasaki Institute of Applied Science, Nagasaki-shi, Nagasaki 851-0193, Japan*
[37]*University of New Mexico, Albuquerque, New Mexico 87131, USA*
[38]*New Mexico State University, Las Cruces, New Mexico 88003, USA*
[39]*Oak Ridge National Laboratory, Oak Ridge, Tennessee 37831, USA*
[40]*IPN-Orsay, Universite Paris Sud, CNRS-IN2P3, BP1, F-91406, Orsay, France*
[41]*Peking University, Beijing, People's Republic of China*
[42]*PNPI, Petersburg Nuclear Physics Institute, Gatchina, Leningrad region, 188300, Russia*
[43]*RIKEN, The Institute of Physical and Chemical Research, Wako, Saitama 351-0198, Japan*
[44]*RIKEN BNL Research Center, Brookhaven National Laboratory, Upton, New York 11973-5000, USA*
[45]*Physics Department, Rikkyo University, 3-34-1 Nishi-Ikebukuro, Toshima, Tokyo 171-8501, Japan*
[46]*Saint Petersburg State Polytechnic University, St. Petersburg, Russia*
[47]*Universidade de São Paulo, Instituto de Física, Caixa Postal 66318, São Paulo CEP05315-970, Brazil*
[48]*System Electronics Laboratory, Seoul National University, Seoul, South Korea*
[49]*Chemistry Department, Stony Brook University, SUNY, Stony Brook, New York 11794-3400, USA*

[50]Department of Physics and Astronomy, Stony Brook University, SUNY, Stony Brook, New York 11794, USA
[51]SUBATECH (Ecole des Mines de Nantes, CNRS-IN2P3, Université de Nantes) BP 20722–44307, Nantes, France
[52]University of Tennessee, Knoxville, Tennessee 37996, USA
[53]Department of Physics, Tokyo Institute of Technology, Oh-okayama, Meguro, Tokyo 152-8551, Japan
[54]Institute of Physics, University of Tsukuba, Tsukuba, Ibaraki 305, Japan
[55]Vanderbilt University, Nashville, Tennessee 37235, USA
[56]Waseda University, Advanced Research Institute for Science and Engineering, 17 Kikui-cho, Shinjuku-ku, Tokyo 162-0044, Japan
[57]Weizmann Institute, Rehovot 76100, Israel
[58]Yonsei University, IPAP, Seoul 120-749, Korea
(Received 16 August 2006; published 16 April 2007)

Differential measurements of elliptic flow (v_2) for Au + Au and Cu + Cu collisions at $\sqrt{s_{\mathrm{NN}}} = 200$ GeV are used to test and validate predictions from perfect fluid hydrodynamics for scaling of v_2 with eccentricity, system size, and transverse kinetic energy (KE_T). For $\mathrm{KE}_T \equiv m_T - m$ up to ~1 GeV the scaling is compatible with hydrodynamic expansion of a thermalized fluid. For large values of KE_T mesons and baryons scale separately. Quark number scaling reveals a universal scaling of v_2 for both mesons and baryons over the full KE_T range for Au + Au. For Au + Au and Cu + Cu the scaling is more pronounced in terms of KE_T, rather than transverse momentum.

DOI: 10.1103/PhysRevLett.98.162301 PACS numbers: 25.75.Dw

Quantum chromodynamics calculations performed on the lattice indicate a transition from a low-temperature phase of nuclear matter, dominated by hadrons, into a high-temperature plasma phase of quarks and gluons (QGP) [1]. For matter with zero net baryon density, this phase transition has been predicted to occur at an energy density of ~1 GeV/fm^3 or for a critical temperature $T_c \sim 170$ MeV [2]. Recent estimates from transverse energy (E_T) measurements at the relativistic heavy ion collider (RHIC) have indicated energy densities of at least 5.4 GeV/fm^3 in central Au + Au collisions [3]. Thus, an important prerequisite for QGP production is readily fulfilled at RHIC. Indeed, there is much evidence that thermalized nuclear matter has been created at unprecedented energy densities in collisions at RHIC [3–10].

Hydrodynamics provides a link between the fundamental properties of this matter (its equation of state (EOS) and transport coefficients) and the flow patterns evidenced in the measured hadron spectra and azimuthal anisotropy [11–15]. Experimentally, such a momentum anisotropy is commonly characterized at midrapidity, by the even order Fourier coefficients [16,17], $v_n = \langle e^{in(\phi_p - \Phi_{\mathrm{RP}})} \rangle$, $n = 2, 4, \ldots$, where ϕ_p is the azimuthal emission angle of a particle, Φ_{RP} is the azimuth of the reaction plane, and the brackets denote statistical averaging over particles and events.

At low transverse momentum ($p_T \lesssim 2.0$ GeV/c) the magnitude and trends of elliptic flow, measured by the second Fourier coefficient v_2, is found to be underpredicted by a hadronic cascade model [18]. By contrast, a broad selection of the data showed good quantitative agreement with perfect fluid (very low ratio of viscosity to entropy) hydrodynamics [9,10,12,15] and a transport model calculation which incorporates extremely large opacities [19]. For higher p_T, quark coalescence from a thermalized state of flowing partonic matter [20–22] has been found to be consistent with the data [23,24]. These results provide evidence for the production of a strongly interacting QGP whose subsequent evolution is similar to that of a "perfect" fluid [7–10].

Systematic theoretical and experimental studies of the influence of model parameters are now required to gain more quantitative insight on the transport coefficients and the EOS for this strongly interacting matter. The range of validity of perfect fluid hydrodynamics is affected by the degree of thermalization [25] and the onset of dissipative effects [25–27]. These questions can be addressed by investigating several scaling predictions of perfect fluid hydrodynamics [15,25,28–30].

In the hydrodynamic model, elliptic flow can result from pressure gradients due to the initial spatial asymmetry or eccentricity $\epsilon = (\langle y^2 - x^2 \rangle)/(\langle y^2 + x^2 \rangle)$, of the high energy density matter in the collision zone. The initial entropy density $S(x, y)$, can be used to average over the x and y coordinates in the plane perpendicular to the collision axis, where x points along the impact vector and y is orthogonal. For a system of transverse size $\bar{R}$ ($1/\bar{R} = \sqrt{1/\langle x^2 \rangle + 1/\langle y^2 \rangle}$), this flow develops over a time scale $\sim \bar{R}/\langle c_s \rangle$, where c_s is the speed of sound. Thus, the initial energy density controls how much flow develops globally, while the detailed development of the flow patterns are largely controlled by ϵ and c_s.

An important prediction of perfect fluid hydrodynamics is that the relatively "complicated" dependence of azimuthal anisotropy on centrality, transverse momentum, rapidity, particle type, higher harmonics, etc., can be scaled to a single function [15,31]. Immediate consequences of this [15,25,28,31] are that: (i) v_2 scaling should hold for a broad range of impact parameters for which the eccentricity varies, i.e., $v_2(p_T)/\epsilon$ should be independent of centrality; (ii) $v_2(p_T)$ should be independent of colliding system size for a given eccentricity; and (iii) for different particle species, $v_2(\mathrm{KE}_T)$ at midrapidity should scale with the

transverse kinetic energy $KE_T = m_T - m$ [15], where m_T is the transverse mass.

We use high statistics v_2 data to test these scaling predictions and explore constraints for the range of validity of perfect fluid hydrodynamics. The measurements were made at $\sqrt{s_{NN}} = 200$ GeV with the PHENIX detector [32] at RHIC. Approximately 6.5×10^8 Au + Au and 8.0×10^7 Cu + Cu minimum-bias collisions were analyzed from the 2004 and 2005 running periods, respectively. The collision vertex z, along the beam direction was constrained to be within $|z| < 30$ cm. The event centrality for Au + Au collisions was determined via cuts in the space of beam-beam counter (BBC) versus zero degree calorimeter analog response [33]. For Cu + Cu only the amplitude of the BBC analog response was used. Charged hadrons were detected in the two central arms ($|\eta| \leq 0.35$). Track reconstruction used the drift chambers and two layers of multiwire proportional chambers with pad readout (PC1 and PC3) located at radii of 2m, 2.5, and 5 m, respectively [32].

The time-of-flight (TOF) detector positioned at a radial distance of 5.06 m, was used to identify pions ($\pi^{\pm}$), kaons ($K^{\pm}$), and (anti)protons ($\bar{p}$)p. The BBCs and TOF scintillators provided the global start and stop signals. These measurements were used in conjunction with the measured momentum and flight-path length to generate a mass-squared distribution [34]. A momentum dependent $\pm 2\sigma$ cut about each peak in this distribution was used to identify $\pi^{\pm}$, $K^{\pm}$ and ($\bar{p}$)p in the range $0.2 < p_T < 2.5$ GeV/c, $0.2 < p_T < 2.5$ GeV/c, and $0.5 < p_T < 4.5$ GeV/c, respectively. A track confirmation hit within a 2.5σ matching window in PC3/TOF served to eliminate most albedo, conversions, and resonance decays.

The differential elliptic flow measurements for charged hadrons and identified particles were obtained with the reaction plane method. This technique correlates the azimuthal angles of charged tracks with the azimuth of the event plane Φ_2, determined via hits in the two BBCs positioned symmetrically along the beam line, covering the pseudorapidity range $3 < |\eta| < 3.9$ [23]. A large η gap between the central arms and the particles used for reaction plane determination reduces the influence of possible nonflow contributions, especially those from dijets [35]. Values of v_2 were calculated via the expression $v_2 = \langle \cos[2(\phi_p - \Phi_2)] \rangle / \langle \cos[2(\Phi_2 - \Phi_{RP})] \rangle$, where the denominator is a resolution factor that corrects for the difference between the estimated Φ_2 and the true azimuth Φ_{RP} of the reaction plane [23,36]. The estimated resolution factor of the combined reaction plane from both BBCs [23] has an average of 0.33 (0.16) over centrality with a maximum of about 0.42 (0.19) for Au + Au (Cu + Cu). The estimated correction factor for the v_2 measurements (i.e., the inverse of the resolution factor) ranges from 2.4 (5.5) to 5.0 (13), for which relative systematic errors are estimated to be ~5% and ~10% for Au + Au and Cu + Cu, respectively.

Figure 1 shows the differential $v_2(p_T)$ for charged hadrons obtained in Au + Au and Cu + Cu collisions. The $v_2(p_T)$ results exhibit the familiar increase as collisions become more peripheral and the p_T increase [3–5]. We test these data for eccentricity scaling by dividing the differential values shown in Fig. 1 by the v_2 integrated over the p_T range 0.3–2.5 GeV/c for each of the indicated centrality selections. The hydrodynamic model predicts that this ratio is constant with centrality and independent of colliding system because ϵ is proportional to the p_T-integrated v_2 values (i.e., $\epsilon = k \times v_2$). The latter proportionality has been observed for Au + Au collisions [37,38]. A Glauber model estimate of ϵ [38] gives $k = 3.1 \pm 0.2$ for the cuts employed in this analysis. This method of scaling leads to a scale invariant variable and cancels the systematic errors associated with estimates of the reaction plane resolution and the eccentricity. It contrasts the methodologies of Refs. [39,40] which calculate ϵ directly for different model assumptions.

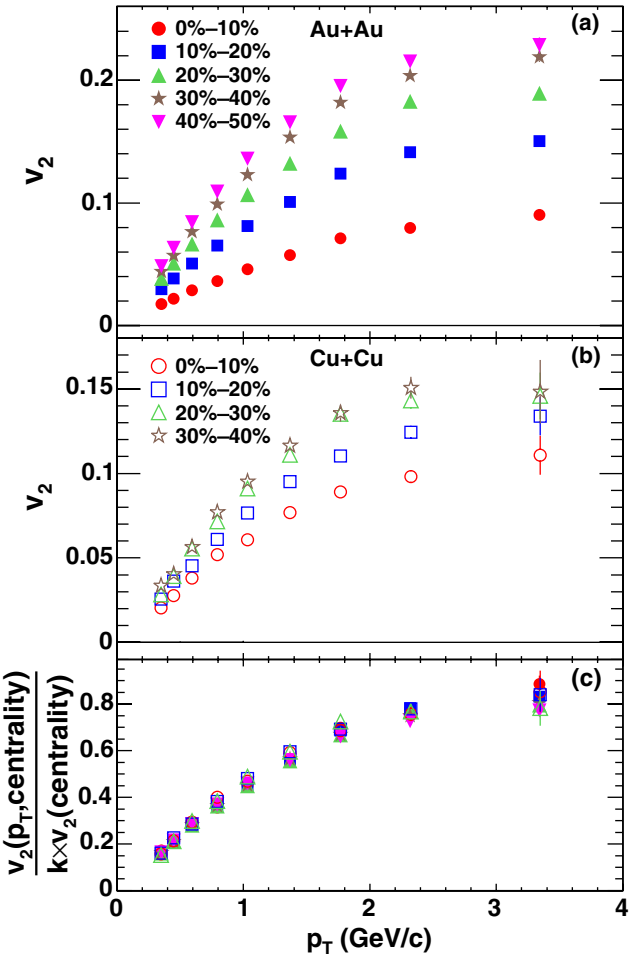

FIG. 1 (color online). v_2 vs p_T for charged hadrons obtained in (a) Au + Au and (b) Cu + Cu collisions for the centralities indicated. (c) v_2(centrality, p_T) divided by $k = 3.1$ (see text) times the p_T-integrated value v_2(centrality) for Au + Au and Cu + Cu.

The resulting scaled $v_2(p_T)$ values for Cu + Cu and Au + Au collisions, are shown in Fig. 1(c). To facilitate later comparisons with the model calculations of Ref. [25], they are divided by $k = 3.1$. These scaled values are clearly independent of the colliding system size and show essentially perfect scaling for the full range of centralities (or ϵ) and p_T selections presented [41]. The scaled v_2 are also in accord with the scale invariance of perfect fluid hydrodynamics [25,29], which suggests that rapid local thermalization [9,10] is achieved. It is noteworthy that similarly robust scaling for the p_T-integrated v_2 is not observed [39,40]. This is probably due to methodological differences in the evaluation of ϵ.

The magnitude of v_2/ϵ depends on c_s [25]. As a reasonable first approximation we compare our measured v_2/ϵ at an integrated $\langle p_T \rangle = 0.45$ GeV/c and the results of Fig. 2 of [25] to obtain $c_s \sim 0.35 \pm 0.05$. Note that this $\langle p_T \rangle$ value accounts for p_T threshold differences and the calculations are done at fixed $b = 8$ fm and constant c_s. Thus, since we expect the speed of sound to vary as a function of time, one might view this c_s value as the approximate average value over the time period $2\,\bar{R}/c_s$, the time over which the flow develops. This value suggests an effective EOS, which is softer than that for the high-temperature QGP [42], but does not reflect a very strong first order phase transition in which matter-flow is significantly slowed or stalled.

Figures 2 and 3 show that the distinctive features of the v_2 for identified particles provide another detailed set of scaling tests. Figure 2(a) shows a comparison of the measured differential anisotropy $v_2(p_T)$, for several particle species obtained in minimum-bias Au + Au collisions at $\sqrt{s_{\rm NN}} = 200$ GeV. The results are in good agreement (better than 3%) with those of our previous measurements [23]. The values for neutral kaons (K^0_s), lambdas (Λ), and the cascades (Ξ) show results from the STAR Collaboration [24,43]. The STAR v_2 values were multiplied by the factor 1.1 to account for a small difference between the average centralities for minimum-bias events from the two experiments. PHENIX and STAR $v_2(p_T)$ results [for $\pi^{\pm}$, $p(\bar{p})$ and K] for 10% centrality bins are essentially identical.

The comparison in Fig. 2(a) shows the well-known particle identification (PID) ordering of $v_2(p_T)$ at both low and high p_T values. At low p_T ($p_T \lesssim 2$ GeV/c), one can see rather clear evidence for mass ordering. If this aspect of v_2 is driven by a hydrodynamic pressure gradient, the prediction is that the differential v_2 values observed for each particle species should scale with KE_T. The pressure gradient that drives elliptic flow is directly linked to the collective kinetic energy of the emitted particles. For higher values of p_T ($p_T \sim 2$–4 GeV/c), Fig. 2(a) indicates that mass ordering is broken and v_2 is more strongly dependent on the quark composition of the particles than on their mass, which has been attributed to the dominance of the quark coalescence mechanism for $p_T \sim 2-4$ GeV/c [22–24].

Figure 2(b) shows the same v_2 data presented in Fig. 2(a) plotted as a function of KE_T. Note that KE_T is a robust scaling variable because it takes into account relativistic effects, which are especially important for the lightest particles. In contrast to the PID ordering observed in Fig. 2(a), all particle species scale to a common set of elliptic flow values for $\mathrm{KE}_T \lesssim 1$ GeV, confirming the strong influence of hydrodynamic pressure gradients. For $\mathrm{KE}_T \gtrsim 1$ GeV, this particle mass scaling (observed for all particle species) gives way to a clear splitting into a meson branch (lower v_2) and a baryon branch (higher v_2). Since both of these branches show rather good scaling separately, we interpret this as an initial hint for the degrees of freedom in the flowing matter at an early stage.

Figure 3 shows the results obtained after quark number scaling of the v_2 values shown in Fig. 2. That is, v_2, p_T, and KE_T are divided by the number of constituent quarks n_q for

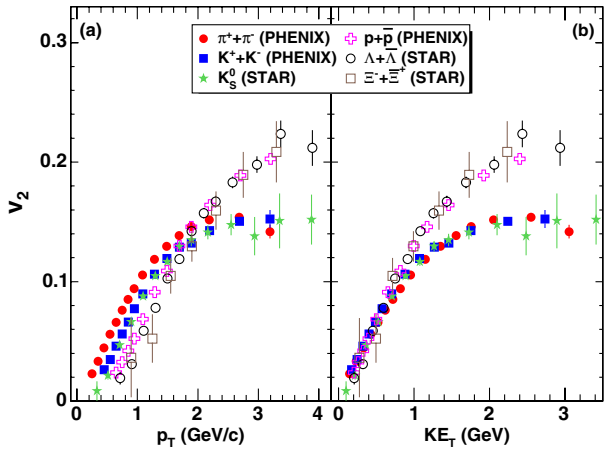

FIG. 2 (color online). (a) v_2 vs p_T and (b) v_2 vs KE_T for identified particle species obtained in minimum-bias Au + Au collisions. The STAR data are from Refs. [24,43].

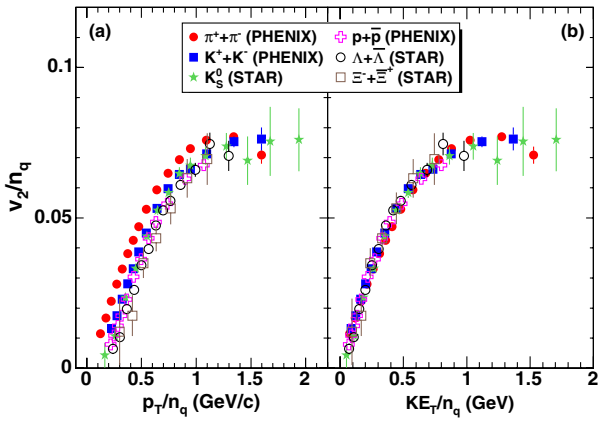

FIG. 3 (color online). (a) v_2/n_q vs p_T/n_q and (b) v_2/n_q vs KE_T/n_q for identified particle species obtained in minimum-bias Au + Au collisions. The STAR data are from Refs. [24,43].

mesons ($n_q = 2$) and baryons ($n_q = 3$). Figure 3(a) indicates rather poor scaling for $p_T/n_q \lesssim 1$ GeV/c and much better scaling for $p_T/n_q \gtrsim 1.3$ GeV/c, albeit with large error bars. The relatively large scaling violation observed for pions indicate that this particle species does not fit the simple quark coalescence picture of Refs. [22–24]. In contrast, Fig. 3(b) shows excellent scaling over the full range of KE_T/n_q values. We interpret this as an indication of the inherent quarklike degrees of freedom in the flowing matter. These degrees of freedom are gradually revealed as KE_T increases above ~1 GeV [cf. Fig. 2(b)] and are apparently hidden by the strong hydrodynamic mass scaling, which predominates at low KE_T. The fact that v_2/n_q shows such good scaling over the entire range of KE_T/n_q and does not for p_T/n_q, serves to highlight the fact that hydrodynamic mass scaling is preserved over the domain of the linear increase in KE_T. Figure 3(b) should serve to distinguish between different quark coalescence models.

In summary, we have presented the results from detailed tests of hydrodynamic scaling of azimuthal anisotropy in Au + Au and Cu + Cu collisions at $\sqrt{s_{\mathrm{NN}}} = 200$ GeV. For a broad range of centralities, eccentricity scaling is observed for charged hadrons for both the Cu + Cu and Au + Au systems. For a given eccentricity, v_2 is also found to be independent of colliding system size. The observed scaling for identified particles in Au + Au collisions, coupled with ϵ scaling, gives strong evidence for hydrodynamic scaling of v_2 over a broad selection of the elliptic flow data. For $\mathrm{KE}_T \sim 1$–4 GeV universal hydrodynamic scaling is violated, but baryons and mesons are found to scale separately. Quark number scaling (v_2/n_q vs KE_T/n_q) in this domain leads to comprehensive overall scaling of the data, with substantially better scaling behavior than that found for v_2/n_q vs p_T/n_q. The scaling with valence quark number may indicate a requirement of a minimum number of objects in a localized space that contain the prerequisite quantum numbers of the hadron to be formed. Whether the scaling further indicates these degrees of freedom are present at the earliest time is in need of more detailed theoretical investigation.

We thank the staff of the Collider-Accelerator and Physics Departments at BNL for their vital contributions. We acknowledge support from the Department of Energy and NSF (U.S), MEXT and JSPS (Japan), CNPq and FAPESP (Brazil), NSFC (China), MSMT (Czech Republic), IN2P3/CNRS, and CEA (France), BMBF, DAAD, and AvH (Germany), OTKA (Hungary), DAE (India), ISF (Israel), KRF and KOSEF (Korea), MES, RAS, and FAAE (Russia), VR and KAW (Sweden) CRDF for the FSU, U.S.-Hungarian NSF-OTKA-MTA, and U.S.-Israel BSF.

*Deceased.
†PHENIX Spokesperson.
Electronic address: zajc@nevis.columbia.edu

[1] F. Karsch, Nucl. Phys. **A698**, 199 (2002).
[2] F. Karsch, E. Laermann, and A. Peikert, Phys. Lett. B **478**, 447 (2000).
[3] K. Adcox *et al.*, Nucl. Phys. **A757**, 184 (2005).
[4] J. Adams *et al.*, Nucl. Phys. **A757**, 102 (2005).
[5] B. B. Back *et al.*, Nucl. Phys. **A757**, 28 (2005).
[6] I. Arsene *et al.*, Nucl. Phys. **A757**, 1 (2005).
[7] M. Gyulassy and L. McLerran, Nucl. Phys. **A750**, 30 (2005).
[8] B. Müller, nucl-th/0404015.
[9] E. Shuryak, Nucl. Phys. **A750**, 64 (2005).
[10] U. Heinz and P. Kolb, Nucl. Phys. **A702**, 269 (2002).
[11] D. Teaney, J. Lauret, and E. V. Shuryak, nucl-th/0110037.
[12] P. Huovinen *et al.*, Phys. Lett. B **503**, 58 (2001).
[13] T. Hirano and Y. Nara, Nucl. Phys. **A743**, 305 (2004).
[14] T. Csörgo and B. Lörstad, Phys. Rev. C **54**, 1390 (1996).
[15] M. Csanád *et al.*, nucl-th/0512078.
[16] M. Demoulins *et al.*, Phys. Lett. B **241**, 476 (1990).
[17] S. Voloshin and Y. Zhang, Z. Phys. C **70**, 665 (1996).
[18] M. Bleicher and H. Stoecker, Phys. Lett. B **526**, 309 (2002).
[19] D. Molnár and M. Gyulassy, Nucl. Phys. **A697**, 495 (2002).
[20] S. A. Voloshin, Nucl. Phys. **A715**, 379 (2003).
[21] V. Greco, C. M. Ko, and P. Levai, Phys. Rev. C **68**, 034904 (2003).
[22] R. J. Fries *et al.*, Phys. Rev. C **68**, 044902 (2003).
[23] S. S. Adler *et al.*, Phys. Rev. Lett. **91**, 182301 (2003).
[24] J. Adams *et al.*, Phys. Rev. Lett. **92**, 052302 (2004).
[25] R. S. Bhalerao *et al.*, Phys. Lett. B **627**, 49 (2005).
[26] T. Hirano and M. Gyulassy Nucl. Phys. **A769**, 71 (2006).
[27] T. Hirano *et al.*, Phys. Lett. B **636**, 299 (2006).
[28] N. Borghini and J.-Y. Ollitrault Phys. Lett. B **642**, 227 (2006).
[29] R. Lacey, Nucl. Phys. **A774**, 199 (2006).
[30] R. Fries *et al.*, Phys. Rev. Lett. **90**, 202303 (2003).
[31] M. Csanad *et al.*, nucl-th/0605044.
[32] K. Adcox *et al.*, Nucl. Instrum. Methods Phys. Res., Sect. A **499**, 469 (2003).
[33] K. Adcox *et al.*, Phys. Rev. C **69**, 024904 (2004).
[34] S. S. Adler *et al.*, Phys. Rev. C **69**, 034909 (2004).
[35] J. Jia Nucl. Phys. **A783**, 501 (2007).
[36] C. Adler *et al.*, Phys. Rev. Lett. **87**, 182301 (2001).
[37] K. H. Ackermann *et al.*, Phys. Rev. Lett. **86**, 402 (2001).
[38] K. Adcox *et al.*, Phys. Rev. Lett. **89**, 212301 (2002).
[39] B. Alver *et al.*, nucl-ex/0610037.
[40] S. Voloshin, AIP Conf. Proc. **870**, 691 (2006).
[41] An apparent difference between these scaled results and those in [38] reflects the fact that eccentricity fluctuations are now taken into account.
[42] F. Karsch, hep-lat/0601013.
[43] J. Adams *et al.*, Phys. Rev. Lett. **95**, 122301 (2005).